International Research Journal of Education and Technology
ISSN 2581-7795

Solar Power as a Secondary Power Source for Electric Vehicles

Tamilarasu R[1], Santhosh K[2], Shankar K[3], Yukesh G[4]

[1]Assistant Professor, [2,3,4]UG Students - Final Year, Department of Computer Science and Engineering, Nandha College of Technology, Perundurai – 638052, Tamilnadu, India

Abstract

Fossil fuels have increased in popularity since the Industrial Revolution in the 18th century, and they are still recognized as an important and ideal source of energy around the world. Global fossil fuel use has increased substantially over the previous century and shows no indications of slowing down, owing mostly to the rising human population and expanding sectors for global economic growth. Earth does not have endless fossil fuel reserves, which will run out soon if we do not reduce our reliance on them. Reducing humanity's dependency on fossil fuels has proven to be a monumental task. This project intends to create a low -cost, environmentally friendly method of transportation that eliminates reliance on fossil fuels. There has been the discovery of an IC Eve Chile (buggy)

1. Introduction

Systems that require expensive new technologies in fact, an EV is more fuel efficient than a conventional vehicle. For a long time, electric vehicles were twice as expensive as gasoline vehicles, and a hybrid was three times as expensive, yet they now cost-despite the fact that the hybrid comprises roughly the same components as a normal car, technology has remained a hobby for enthusiasts. The reasons for this are several, but one of the most important is the availability of an electric automobile at a comparable price. It's likely that the technology has always been more expensive than traditional methods. Hydrogen power is appealing since it can be used to refuel cars, and there are always new uses for it.

The United States today has bipartisan support for creating infrastructure for the electrification of its transportation system for national security reasons. It is debatable that the country cannot spend trillions of dollars each year importing fuel from all over the world when doing so would endanger the country's economy and exacerbate the problem. Even at this early stage, it is clear that the cost will be large-perhaps US$200 billion-but this cost is a small fraction of what gasoline would cost in the future if nothing is done.

An electrified transportation fleet has advantages: it can run on almost any fuel, wind, solar, nuclear, woody biomass, tidal, wave and it is easy to keep its carbon free or at least carbon neutral. Dynamic demand control (DDC) of the grid means that energy can be fed into the grid system when it is available and the electric vehicle fleet will vary its uptake dynamically to maintain the grid and improve the quality of power to all other users. There is no other power application of such magnitude that can control the grid and improve the power quality while allowing renewable energies to feed directly into the network. Further, bidirectional chargers allow the batteries of stationary EVs to act as an energy store for the grid and supply peak power as required. With a large number of EVs, the energy storage can be very high but the economics of this technique must balance the cost of the scheme against the cost of cycling the batteries.

Over the last 20 years, hardware to establish an electrified transportation system has been presented in publications. Early US patents such as 4331225, 4836344, and 6879889, among others, propose allowing vehicles to pick up power inductively while driving (now known as Dynamic Inductive Powered Transportation (DIPT)), but none have been implemented to date because the technology lacked utility and was not cost competitive with gasoline. These disadvantages are no longer applicable, and extensive research over the last decade has resulted in systems that can power moving vehicles over adequate air gaps at levels required by modern EVs, using both single and multiphase systems. Coils are arranged in a continuous strip along the road in such systems. This strip is followed by a vehicle.

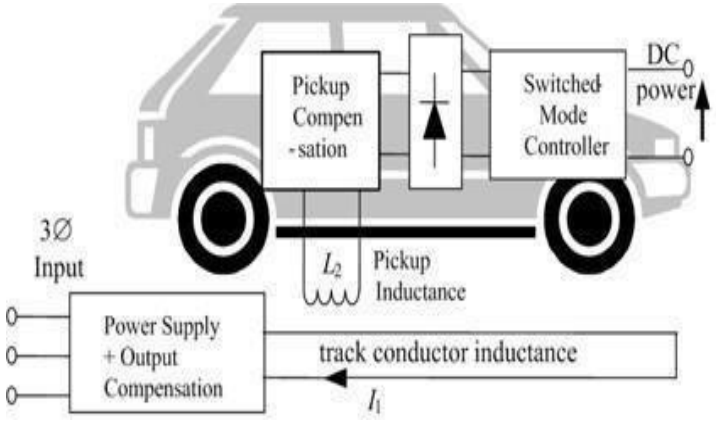

Figure 1 A typical IPT system

Increasing the power and separation between the track and the receiver on the vehicle is desirable for air gaps of 100-300mm. A well-designed system is in general tolerant to misalignment and variable air -gap lengths bus systems. Hardware to build an electrified transportation system has been presented in the with roadway applications, such variations are likely to be extreme and some mechanisms may be needed to help with automatic alignment. This paper presents both simulated and experimental measurements on technology for roadway-powered electric vehicles, including measurements for a wind -powered system operating with an inductive power charging system at a laboratory scale.

2. System Overview

2.1 A Possible IPT Roadway System

Electric vehicles reduce dependence on fossil fuels and emission of greenhouse gasses and pollutants. Consequently, EV uptake has been increasing however market penetration has been low because EVs are less cost effective than conventional vehicles. The present EV market is dominated by hybrid vehicles that derive their energy from an IC engine, but, plug -in EVs (PHEV) were recently introduced enabling grid energy to mitigate gasoline consumption. For E Vs. to gain widespread adoption, major improvements are required in battery life and cost, and grid connection. Instead of a single continuous daily charge, the latter allows for opportunistic recharge after each excursion. By reducing the depth of discharge, battery wear is greatly decreased, and the EV costs less because a smaller battery is required.

As described, the recommended approach for making electric vehicles more cost effective than gasoline vehicles is to power and recharge them on the road. Because interstate roads account for only 1% of all roadway miles but carry 22% of all vehicle miles driven, the infrastructure for such a dynamic charging system might be relatively small. An EV that is connected to a dynamic charging system for 50% of its driving kilometres is as cost -effective as a conventional vehicle. The purpose of this research is to investigate a practical Inductive Power Transfer (IPT) system powering and recharging EVs moving along a roadway, completely minimizing on board energy storage and hence vehicle weight and cost. Fig. 2 shows a possible configuration of such a highway system. Power supply cabinets can be placed alongside the highway at suitable spacing (say 20200m). Within each cabinet, there exists one or more suitable resonant power supplies capable of energizing one or more pads placed along the centre of a highway lane. Only pads that are underneath a vehicle that can receive power from the roadway should be energized. This ensures that other vehicles can travel along the roadway without acting as an undesirable load and that conventional vehicles are not heated by magnetic fields. To transfer sufficient power one or more pads sitting underneath a moving vehicle will need to be energized, requiring suitable detection means for the position of the vehicle, and means to switch roadway pads on and off sequentially, while supplying each with an appropriate current.

In diverse settings such as urban, highway, and hilly terrains, a power input of 10 -30kW to an EV is suitable for motive power and charging while driving. The amount of energy gathered by the EV is determined by the length of the powered road and the speed of the vehicle. Furthermore, placing powered parts on steep sections of route is ideal to limit the car battery's discharge rate and extend its life. Each pad in the DIPT system presented here should be capable of delivering at least 10kW to a vehicle and be no more than one or two metres square. As a result, larger vehicles may require the use of two or more pads to receive higher power transfer rates. Furthermore, while IPT systems have been discussed for some time, large -scale systems have to date appeared impractical due to the challenge of coupling such power with large horizontal tolerances (~±350-±700mm) while meeting ground clearances of 100-300mm required by various EVs. For North American highways there is a further demand, in that any pad on the road must be covered by 50-75mm of asphalt. Naturally, the focus over the last decade has therefore been on lumped systems for EVs at modest power levels (2 -3kW) for home-based charging. The magnetic designs of such systems are naturally focused on power transfer at a defined location, and often assume some guided assistance for parking. The challenge is how to ensure these magnetic designs are future -proofed and suitable for both stationary and moving applications. The following section discusses recent magnetic developments for EV charging and focuses particularly on those that could be scaled to the levels now required.

With today's Power Systems there is an increasing emphasis on 'green' power achieved using renewable sources with little or no carbon footprint. Such sources include wind, wave, and tidal power all characterized by being fluctuate to such an extent that the power from them cannot be guaranteed even for only a few minutes into the future. These sources are important as they are carbon free but their use means that the grid frequency cannot be held as precisely as has now come to be expected. Electric vehicles will therefore at various times be driven by green power when parked charging, or when moving powered by IPT where they must maintain their roadway position at the required speed. There are two fail -safe conditions that the home or roadway-based power supply must meet: a situation where grid power is temporarily not available, and a situation where the power required exceeds the rating of the power supply. Variations are many and include the condition where a large surge of power is available and vehicles may use it to charge their batteries, even though it is only a temporary surge.

There are current proposals for solving the power system problem. It has been suggested that all PHEV chargers could be fully reversible so that when the vehicle is parked up and charging overnight the electricity company can reverse the charging process and drain energy from the batteries of all the vehicles on a charge to meet temporary power demand. Such a power reversal would need significant communications over a whole country/region and would have to be very fast acting to avoid spectacular collapses as the power system becomes overloaded. As more generators drop out the frequency decreases more rapidly and the condition worsens. If all the reversible battery chargers could be reversed the process might be saved but such power reversal would have to occur very quickly — probably in less than 5 seconds - in the collapsing power system to save it. With DDC implemented within the home-based charging and roadway network, this problem is mitigated. When the power system has a lot of wind power added to it at times of wind surges the mains frequency will increase slightly and with DDC implemented this will signal the battery charging to increase where possible.

Conversely when the wind dies the charging can be reduced, and even with dynamic charging the battery energy will easily provide a ride-through period. In concept, if upwards of 20kW is being transferred to each vehicle along a highway and this is split evenly (10kW for motive power and 10kW for charging), up to 10kW/vehicle can be instantly shed (that is required for charging) without affecting the battery on board battery capacity. A further 10kW/vehicle may be available providing the on board battery is sufficiently charged to be able to be discharged for the period required. As a result, an EV system with DDC power supplies and batteries will increase the quality of supply with wind generation by assisting in frequency stabilisation. In Figure 3, traditional generators service typical consumer loads, but energy-based loads such as electric vehicles (EVs) are used to capture variable energy from fluctuating sources such as wind. This topic is explored further in the fourth section. Throughout the electricity system, boost the use of renewable energy.

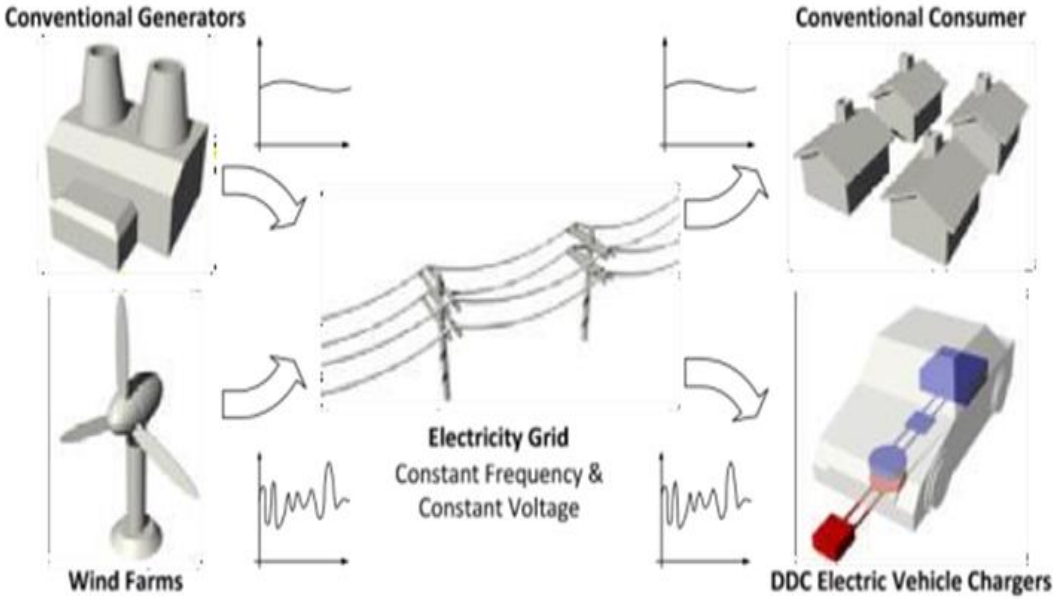

Figure 2 DIPT can be improved with DDC to improve

3. Charging Pad Developments for EVS

3.1 Single Phase Charging Pads

The most common inductive charging system proposed to couple flux between a primary transmitter and secondary receiver has a circular magnetic structure. Both the ground and receiver pad are nominally identical. Each has six main components shown in the exploded view of Fig. 4. The aluminium ring and backing plate shield the chassis of the EV and the surrounding area from stray magnetic fields. Alternative power couplers are; pot cores, U-shaped cores, ferrite discs or plates or E-cores. All of these are comparatively fragile and expensive due to the geometry of the large pieces of ferrite required to achieve the desired power transfer flux path. Arrays of coils with ferrite backing allow power transfer over large areas with low power systems however this technique is not cost effective for high er power EV charging systems. As shown, each row or column of coils needs to be switched to prevent field cancellation in the centre of the multilayer array to increase the power transfer - this is impractical with high power systems. Coreless coils as shown are generally not suitable for high power applications with conductive or ferrous materials close to the system. Field shaping with ferrite constrains flux to desired paths improving coupling and preventing excessive energy loss in surrounding materials. As shown, the mutual inductance between couplers and the primary current has the greatest influence on power transferred. To compensate for lower coupling and maintain good efficiency, coreless systems are operated in the MF to VHF bands efficient operation at such high frequencies is not possible at high power due to limitations with current semiconductor devices.

The Power Pads overcome several limitations of common couplers by using multiple smaller bars held in place by a shock absorbing coil former with further protection provided by the aluminium and plastic case. Power pads are thin compared to standard core topologies and are lighter than conventional circular coupler designs that use solid ferrite discs. A 2kW pad system capable of operating with an air gap of approximately 200mm was presented. Here the length of the ferrite bars was the most important factor relating to the ability of this structure to achieve the necessary separations desired (in this case the pad was optimized for 2 00mm separation). This resulted in a 700mm diameter pad constructed with twelve ferrite spokes made up of three standard ferrites 'I' bars (93mmLx28mmWx16mmT). The coil consists of 25 turns of 4mm diameter Litz wire. The measured and simulated performance at 20 kHz with a current of 23A is shown in Fig. 5. With the PSU shown it can deliver 2kW with Q<5 within ±100mm, but for larger tolerances, a much larger pad would be required. Furthermore, flux is launched from the centre of the transmitter pad to r return at the outer edge of the pad so that the field lines only extend upwards to a useful height of approximately ¼ of the pad diameter. For roadway applications, significantly larger pads would be required. Finally, if circular pads were placed side by side along a highway as indicated there would also be unavoidable nulls in power transfer between pads so that each pad would have to transfer peaks of twice the average power demand to ensure adequate power transfer. These fundamental limitations mean that t circular pads are not suited for a dynamic roadway system.

To overcome the shortcomings of the circular pad structure, a new battery charging magnetic structure using bars has been proposed. This bar pad structure creates essentially a horizontal flux profile compared with the vertical fields of the circular pads as shown in the comparisons of Fig. 6(a) and (b).

The advantage of this structure is that the field naturally achieves a higher height and therefore the coupled power to a receiver designed to capture the horizontal (rather than vertical) field is improved. The coupling factor, κ, provides a useful measure for comparing the magnetic properties of different pad topologies. The track and receiver pads of these charging structures are typically constructed to have an almost identical magnetic structure. For evaluation, each pad can be made to have the same number of turns, although in practice the turns will be chosen based on output current and voltage demands. Improved coupling significantly increases the system efficiency and power transfer at a given current and frequency as indicated. The design of the flat pad is significantly improved if a flux pipe is introduced as shown in with coils placed at either end to drive the flux from one pole through the ferrite bar structure to the other pole end. The pole ends are then designed to efficiently launch and capture the flux to achieve good coupling.

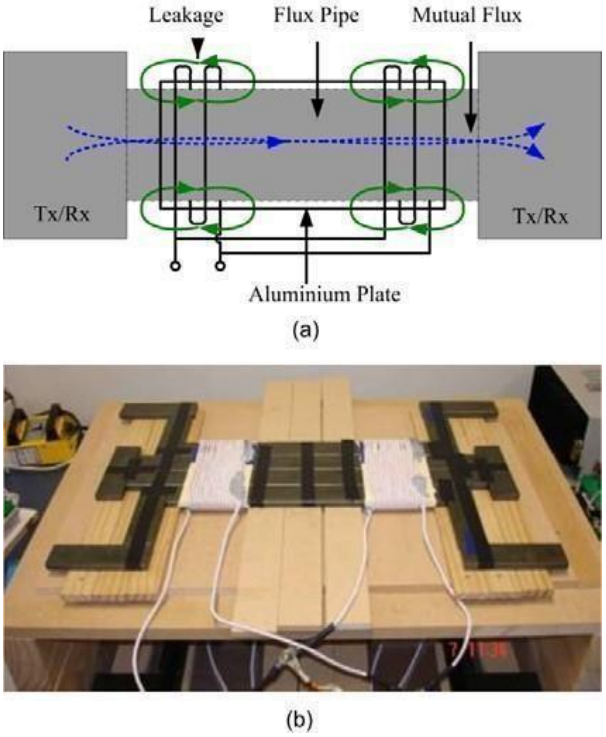

Figure 3 A horizontal flux pads with flux pipe (a) concept with coils in parallel (b) prototype flux pipe with two 15 turn coils

A comparison of this new “flux pipe” pad against a 700mm diameter circular pad is shown in Table 1 and Fig. 8, with both pads excited at 20 kHz and 23A. This new pad uses essentially the same number of ferrites, but only 42% of the wire, and therefore copper losses are significantly reduced. This "flux pipe" pad structure of Fig. 7 is polarized, unlike the circular pads, described earlier, and therefore comparisons need to be made in terms of offsets in all x, y, and z axes. The area of the pad being significantly smaller, the results show a clear improvement in coupling factor for vertical (z) separations above 120mm (Fig. 8(a)) and at the desired 200mm separation point, significantly better coupling for all lateral offsets in the x or y directions (Fig. 8(b)). The uncompensated power (PSU) at 200mm separation (from Table 1 below) is superior, clearly indicating that the f lux pipe is a lighter and more cost -effective design. Furthermore, this flux pipe design allows 2kW to be transferred within a ~200mm radius of the pad centre, which is a significant improvement.

The ferrite is utilized far more effectively in the flux pi pe and the power transfer density is significantly higher allowing compact pads that simplify mounting on EVs. The power drops off slowly in the y axis (along the direction of the highway), so that if these pads are placed along a highway and configured such that they are driven synchronized, in phase, then it is possible to deliver a power profile that is always available to a vehicle without the power nulls that would arise from cascaded circular pads. Power transfers of 10kW can be achieved by increasing the pad current and operating frequency, but achieving this with a very large horizontal (x) tolerance is still demanding. An alternative approach with significantly improved horizontal tolerance using a multiphase pad is as described following.

3.2 Pads for Multiphase Charging

A bipolar three-phase track topology was developed to increase horizontal tolerance. A three -phase inverter drives overlapping phase wires on this track. Due to the overlapping structure of the track phases, currents in nearby wires differ by 60 degrees, similar to windings in a cage induction motor. This forms a travelling field over the track, resulting in a wide and even power profile that can be captured with a simple receiver pad. Similar to the flux pipe explained in the preceding section, such a simple receiver captures horizontal flux. Mutual inductance between phases is, however, a side effect of having overlapping tracks. This means that energy from one track phase can couple into neighbouring phases, similar to how power is transferred between track conductors and receivers. It is possible, though costly, to solve this problem.

Alternatively, a unipolar three -phase track topology structured as in Fig. 9 can be used (named because there are no explicit return conductors). Notably, the horizontal tolerance of the receiver is now determined by the width of the track rather than simply it is resonant current rating. Increasing tolerance requires making the track wider and this added length increases the copper loss linearly. A range of parameters affects the output power of such a system, including the magnetic length, width, and thickness of the receiver pad, the track pitch and width, and the design of the ferrite structure under the track. These were investigated by simulation and reported, resulting in a prototype design for a pad for the DIPT system. The pad operates with an air gap of z = 175mm. In this evaluation, the receiver is simplified to that of a simple bar with a single winding to aid analysis. Results show that if it is made to be four times the pitch of the track with a winding that covers around 80% of the receiver ferrite almost all of the available horizontal flux is captured. The total track width evaluated was 1550mm, corresponding to a midsection width of 800mm and a pitch of 250mm. The receiver was therefore 1m long and had a width of 0.3m. Ferrite is also required underneath the track to enhance coupling. Various options were considered from a full ferrite sheet to ferrite strips. Eight 20mm wide ferrite strips with a relative permeability of 2000 placed equidistantly under the straight section of the track were found to give good performance.

The resulting power profile is shown in Fig. 10. Here the track current/phase was set to 250A which is typical for industrial IPT systems. The chosen frequency was also increased to ~40kHz. Each line represents the available PSU with the receiver positioned at z=175mm separation but various offsets from the canter and moving in the y direction (along the track) over a length equal to a full 360° movement. Here x=0mm represents operation along the track centre, while an x=400mm offset represents operation while moving close to the edge of the track where the wires loop back. As expected, power falls off dramatically at this point, as flux essentially cancels. The small ripple showed results from the curved end sections. If a Q of 5 is permissible, a continuous 30kW can be linked to an EV over an 800mm wide zone if required.

3.3 A Possible Stationary and Dynamic System

From the above results, it seems feasible that a DIPT system could be created for EVs. The vehicle would be fitted with one or more relatively simple receiver pads (such as the flux pipe receiver described earlier) placed underneath. Such a pad can couple power and receive a charge when the EV is parked stationary over a similar "flux pipe" power pad on the ground, but can also couple power dynamically from a roadway system constructed of either single or multiphase power pad structures as described above. As shown, these systems have both horizontal and vertical components of flux in both single and multiphase systems, so that systems can benefit if a quadrature (essentially two phases) power receiver is used, rather than the simple horizontal flux receiver described for the flux pipe or bar shaped receivers. This only requires a second coil configured to capture the vertical flux and suitable processing electronics.

4. Charging using Dynamic Demand Control

4.1 Dynamic Demand Control Concepts

To evaluate the advantages that DDC could bring, an IPT battery charging system operating from single phase mains with DDC was developed for evaluation purposes. The system is shown conceptually in Fig. 11. The power supply presented was used here. It outputs a regulated current at a fixed frequency of 20 kHz into the ground pad of the battery charger system. This power supply has minimal DC energy storage, good input mains power factor, and efficiency. A feature of the e power supply is that the DC link in the power supply, and hence the track current I1, is amplitude modulated at twice the mains frequency due to the minimal DC energy storage. For DDC the pick-up controller topology needs to be able to regulate its output t power continuously or in multiple small steps like those discussed. An LC parallel tuned AC -AC pick-up controller presented is used simply because it has high efficiency and fast response, and the capability to vary the output power continuously from no load to full load. The primary and secondary charging pads used in this system are the circular lumped coil types as discussed in section 3.1 and presented.

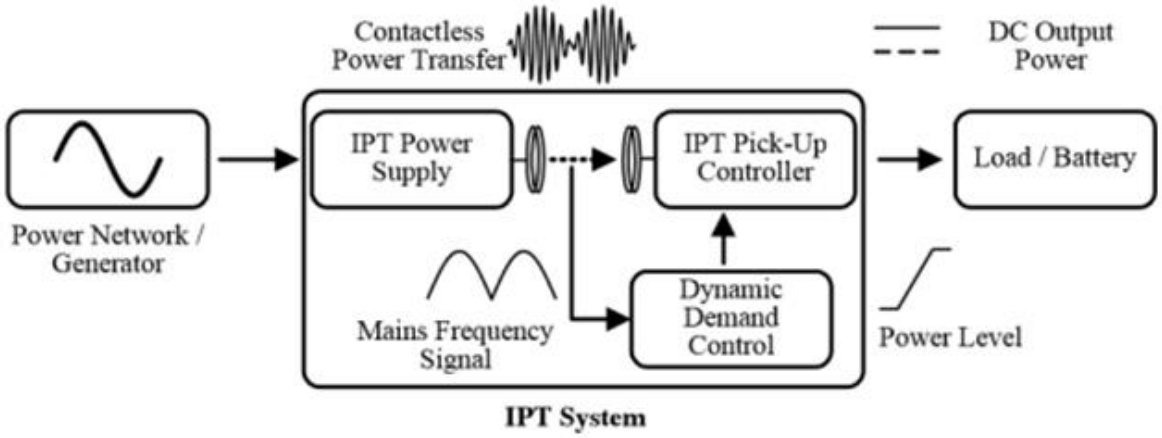

Figure 4 Overview of an IPT charging system with DDC

The role of the dynamic demand controller is to send the desired output power level to the pick -up controller based on the measured grid frequency. The frequency window used in this system is set but not limited to 49.5—50.5 Hz. In this range, the battery charging system should operate linearly from no load to full power as shown in Fig. 12. As the primary track current envelope is amplitude modulated at the grid frequency, the induced voltage in the secondary is also modulated enabling the grid frequency to be simply measured on the secondary (vehicle) side without complicated circuitry. For systems with constant track current envelopes, an alternative method would be needed.

4.2 An Evaluation System

A simple block diagram of the global control system is shown in Fig. 11. It comprises a power network/generator (without any governor action) and a battery charging system.

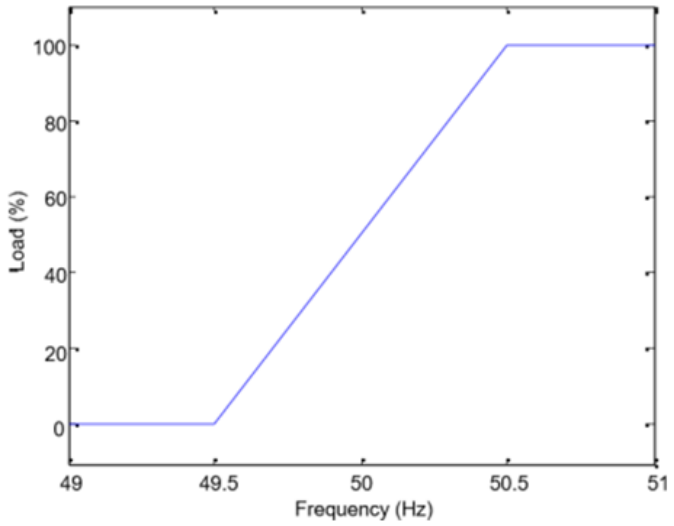

Figure 5 Output power and frequency characteristic with DDC

In the block diagram, the power network is simply modelled as a rotational body with inertia J (Nm 2), and "k" is a droop factor (Nm/(rad/sec)), which is essentially the slope of the line in Fig. 12. For the example shown, the line rises from zero to rated torque in 1Hz or 2% of rated speed. For a 2-pole generator rated at 7.5 kW used here for the laboratory measurements, "k" would be 25 Nm/6.28 radians/sec or approximately 4 Nm/(rad/sec). T is the frequency measurement time constant and as shown is assumed to be that of a first order system. Without the battery charging system, any torque variation ($\Delta\tau$) applied to the generator results in a system frequency deviation ($\Delta\omega$) (assuming a constant consumer loading condition). Using the dynamic demand control IPT system, $\Delta\tau$ is then reduced from the power network/generator by varying the power delivered to the load/battery according to $\Delta\omega$. This results in an appropriate change to the grid frequency keeping it within the present window.

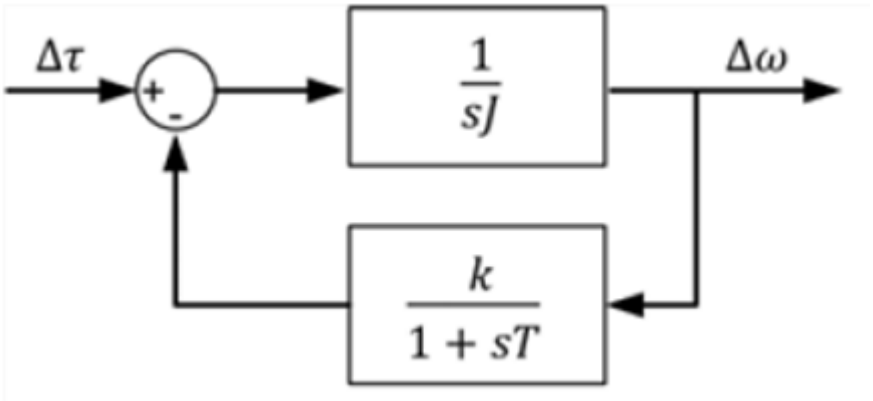

Figure 6 Block diagram of the control system

Thus, for the 2-pole generator as above, assuming small system inertia of 0.35 kg.m^2 and a 100 ms. the filter time constant, the damping factor is 0.47, the settling time is approximately 0.3 s and the speed offset is 0.25 radian/sec/Nm. This example considers but a tiny system — corresponding to the experimental example following. Larger systems would have much higher inertias giving better damping factors but the same offset dependent on the slope of the line in Fig. 12. To get a faster response the measurement time constant may be reduced but this leads to a significantly worse damping factor. To measure the performance of the frequency measurement technique, the proposed battery charging system was driven from a single-phase variable frequency AC supply (Agilent AC power source 6813B) with the system operating under full power conditions. The frequency varied slowly from 49.5 Hz to 50.5 Hz. Partial measured results are presented in Fig. 14 (upper trace) where it is apparent that individual measurements are significantly affected by noise. To improve this, the measured results were filtered using a rolling average of eight measurements after which a frequency variation of 0.01 Hz is now discernible as shown in Fig. 14 (lower Trace).

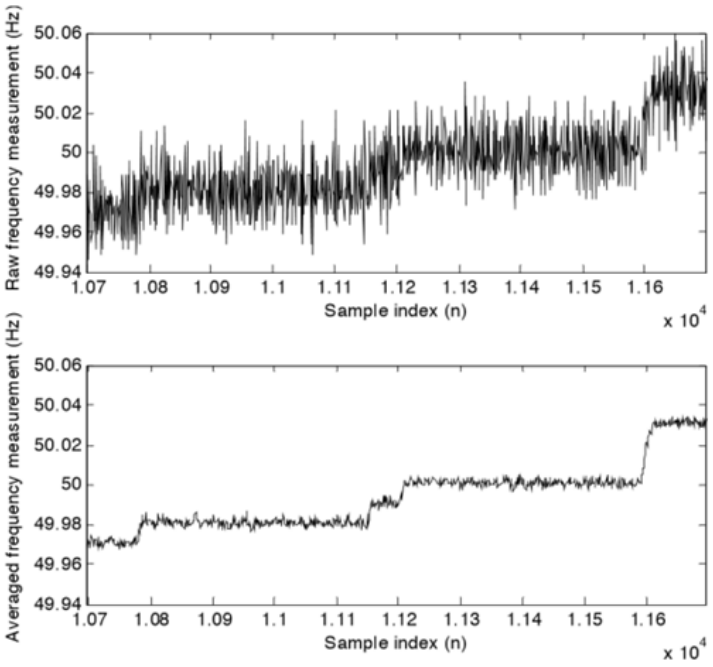

Figure 14: Raw frequency measurements (top) and averaged frequency measurements (bottom)

For evaluating the performance of the dynamic demand control IPT system, a programmable standalone power generation system was constructed comprising a variable speed drive (VSD), a 3-phase induction motor, and a 3 phase AC generator. This system was set up to generate 230 V 50 Hz (per phase) and is capable of delivering up to 7 kW total. The IPT charging system was connected to one phase, while constant resistive loads were connected to the remaining two phases to emulate a constant consumer load demand. To emulate a power network with high penetration of time-variable renewable energy sources (e.g., wind energy), the VSD was configured to operate the induction motor in a torque-controlled state where the desired speed was set to the maximum value but the actual speed is limited by the torque demand. Changes to the torque -demand cause the generator to accelerate or decelerate. A random but repeatable pattern of torque commands with a distribution close to a Weibull pdf was used as the torque input to the VSD as shown in the top trace of Fig. 15. In this way, a highly variable isolated power system with statistical properties close to that of wind was created with the ideal feature that the numerical sequence could be repeated to make different measurements on the same data.

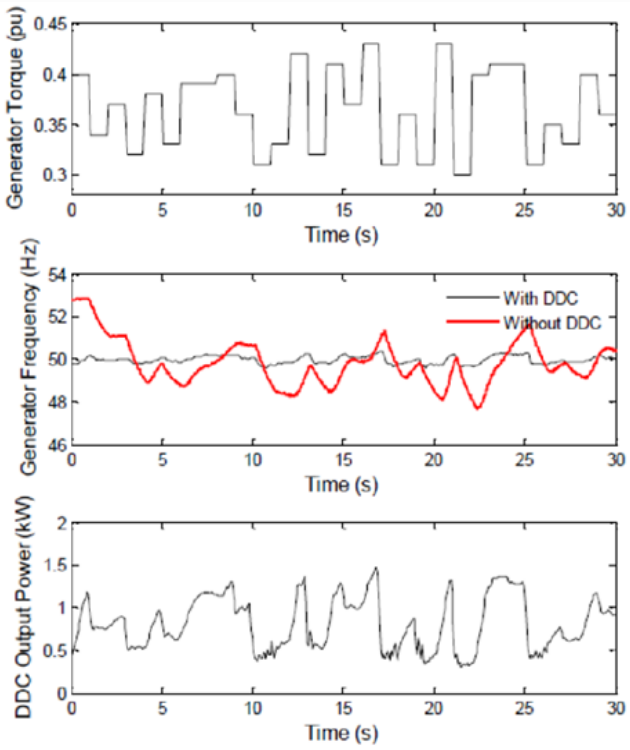

Figure 15: Measured generator frequency and charging system output power (middle and bottom) when the motor-generator set is driven with a random torque pattern (top)

The system was operated in a steady—state model and a sequence of 50 random torques was input to the VSD at one-second intervals to emulate a changing wind pattern with the dynamic demand IPT battery charging system connected to the generator, the system frequency of the generator and the output power of the charging system was then measured under battery charging conditions. Using an identical torque sequence, the system frequency was also measured with the battery charger behaving like a static load (without DDC). The measured results from the 30 seconds.

Without DDC in place, the measured generator frequency is unstable and varies from 47 Hz to 53 Hz. By any measure, this is a power supply of very low quality and has limited usefulness. By comparison, with DDC employed (as shown on the same traces in Fig. 15 and 16 for comparison), the frequency of the generator is successfully maintained within the present window of 49.5 to 50.5 Hz. A comparison of the torque pattern input to the generator and the output power profile of the charging system of Fig. 15 (bottom trace) clearly shows how closely the output power profile follows the input torque pattern. As the torque limit of the induction motor is increased, the frequency speeds up but the charging system absorbs this excess power and removes the excess torque from the generator to roughly maintain the system frequency. Conversely, as the torque limit is decreased, the generator slows down forcing the charging system to reduce its power consumption, thereby reducing the total frequency change.

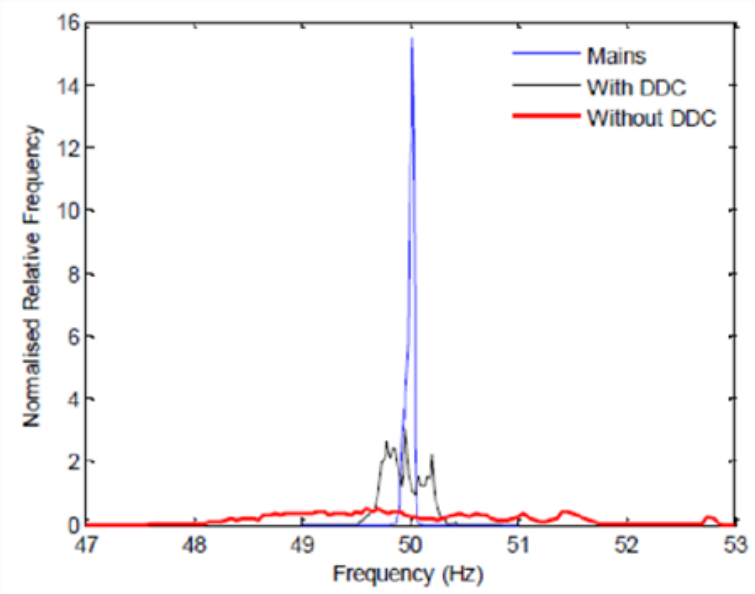

Figure 16: Generator frequency distribution with and without DDC

The findings of the dynamic demand control experiment with an emulated fluctuating power network show how a DDC-controlled IPT battery charger may provide significant frequency smoothing by altering its output power in response to supply frequency discrepancies. Large -scale deployment of battery EVs with DDC chargers could act as a dispersed load that increases the reliability of any supply network without the requirement for expensive high bandwidth centralised communication infrastructures. This lowers the amount of spinning reserve governor activity required and promotes wind power penetration without significantly increasing grid demand-supply balancing costs. However, as described, attention must be made to examine the regional supply -and-demand balance to avoid an unwelcome rise in TimeLine flow. This approach can theoretically be utilised on very large roadway systems with moving vehicles.

5. Conclusions

As shown in this paper, it is now technically feasible to supply power to moving EVs such that the on board battery can be significantly reduced. The system introduced here is fully modular and widely applicable and allows the grid to extend to the roadway which provides the lowest cost EVs of all possible architectures. Wind or other green power can be wheeled through the grid to allow the dynamic battery load to match generation to demand in the rest of the network. The future enhancement encloses the voice control car using solar power.

References

1. Choe, G.Y., Kim, J.S. and Lee, B.K. 2010. A Bi -directional battery charger for electric vehicles using photovoltaic PCS systems. In: IEEE Vehicle Power Propels Con f., IEEE, pp. 1-6.

2. Spina, M.A., de la Vega, R.J., Rossi, S.R., et al. (2012) Source Issues on the Design of a Solar Vehicle Based on Hybrid Energy System. International Journal of Energy Engineering, 2, 15 -21.

3. M. Azeoual et al., "Renewable Energy Potential and Available Capacity for Wind and Solar Power in Morocco towards 2030," Journal of Engineering Science and Technology Review, vol. 11, no. 1, pp. 189-198, 2018, 10.25103/jestr.111.23.

4. M. Inchaouh and M. Tahiri, "Air pollution due to road transportation in Morocco: Evolution and impacts," Journal of Multidisciplinary Engineering Science and Technology, Vol. 4, no. 6, pp. 7547-7552, 2017.

5. M. M. Erdogdu et al., "Renewable Energy Sources: Comparison of their Use and Respective Policies on a Global Scale," in Handbook of Research on Green Economic Development Initiatives and Strategies, 1 st ed. IGI Global, 2016, ch. 11, pp. 238 -269.

6. AnyosJedlik, Electric Vehicles History Part II, Early History, 1998, the invention of the Electric vehicle, Accessed April 2017

7. Yogesh Sunil Wamborikar, Abhay Sinha ―Solar powered Vehicle‖, WCECES Paper 2010.

8. Fattori, F., Anglani N. and Muliere G. 2014. Combining photovoltaic Energy with electric vehicles, smart charging and vehicle-to-grid. J. Solar Energy, 110: 438-51.

9. ESVC 2016, Rules and Regulation of ESVC 2016.

10. Goli, P. and Shireen, W. 2014. PV powered smart charging station for PHEVs. J. Renewable Energy, 66: 280 -7.

11. Thirugnanam, K., Ezhil Reena, JTP., Singh, M. and Kumar, P. 2014. Mathematical modelling of Li -ion battery using genetic algorithm approach for V2G applications. IEEE Trans. Energy Convers. 29: 332-43.

12. Singh, M., Thirugnanam, K., Kumar, P. and Kar, I. 2015. Real -time Coordination of electric vehicles to support the grid at the distribution Substation level. J. IEEE Syst., 9: 1000 -10. Doi.org/10.1109/ JSYST.2013.2280821.

13. Capasso, C. and Veneri O. 2015. Experimental study of a DC charging Station for full electric and plug in hybrid vehicles. J. Applied Energy, 152: 131 -42.

14. "Solar vehicles and benefits of the technology", by John Connors, ICCEP paper 2007.